TWO-AND THREE-DIMENSIONAL ANALYSIS OF PENETRATION AND PERFORATION

T. Maini* and M. L. Wilkins**

Principia Mechanica Ltd., 50 Vincent Path, East Sheen, London SW14 8LL, England
University of California Lawrence Livermore Laboratory, Livermore, CA 94550, USA

ABSTRACT

The numerical procedures used in the computer codes HEMP and PR3D to simulate penetration and perforation are described. Both programs use dynamic, non-linear finite difference formulations and an explicit time integration scheme. The formulation in HEMP is two-dimensional, while PR3D can analyse three-dimensional situations. Non-linearities can be either constitutive or geometric. The latter includes large strains. Propagation of fracture is simulated by representing advancing cracks as element-wide bands.

Examples demonstrating both theoretical aspects and practical applications of impact and perforation problems are also presented. The examples include the impact of a missile on armour plate and the perforation of a roof plate by a pipe-end.

KEYWORDS

Impact, penetration, perforation, dynamic analysis, finite differences, ductile fracture.

INTRODUCTION

Impact between two objects will result in partial or complete penetration and possibly fracture of material. When penetration is complete, it is referred to as perforation. There are several fracture mechanisms that may occur during perforation (Wilkins, 1978). The most common are spall, hole enlargement by radial flow, plugging and petaling. The actual mechanism that operates depends on (Johnson, 1972) the speed and angle of impact, material properties of both target and missile, shape of the projectile nose, the projectile diameter to plate thickness ratio and the support conditions of the target.

The authors have used the finite difference programs HEMP (Wilkins, 1969) and PR3D (Principia, 1983) to investigate situations involving impact and penetration. These investigations have assisted the determination of which of the factors mentioned above influence specific fracture mechanisms and have also permitted the analysis of realistic impact configurations which could not be assessed using simple analytical techniques. It is extremely difficult to obtain reproducible experimental results using projectiles at speeds of 1000 metres per second and it is this that makes the use of computer simulation programs such as PR3D and HEMP particularly attractive.

In the subsequent sections, we will describe the numerical formulations used in the two computer codes to represent the continuum behaviour of material, the interaction between two objects and the propagation of fracture. The remaining sections consist of applications of PR3D and HEMP to both two- and three-dimensional problems. Some of the examples will help to explain features of penetration and perforation, thus demonstrating the insight that can be gained by the use of such codes. Other examples describe practical situations that have been investigated by the authors and their colleagues.

Here, we are concerned with impact velocities of less than 3km/s. In this range, penetration mechanisms are controlled by the inelastic behaviour of the interacting bodies (Wilkins, 1978).

CONTINUUM FORMULATION

Impact problems are characterised by a short duration and a strongly non-linear behaviour. The latter arises from geometric non-linearities associated with the establishment of contact between bodies and also from the levels of deformation induced in the material as impact velocities are far greater than that needed for yield. Explicit time integration of the equations of motion is the method most suited to the solution of such problems. The non-linearities can be handled easily as iterations are avoided and fracture can be treated simply, although the size of the timestep is limited so that no nodes can communicate physically during one timestep. The analysis therefore proceeds in cycles. Each cycle is typical and performed repeatedly until the timespan of interest has been covered. Both HEMP and PR3D use explicit time-marching techniques and can be used for two-and three-dimensional analyses respectively.

Both missile and target objects are represented by meshes of constant strain elements with masses lumped at each node. The mesh is continuously updated during the calculation to represent the deformed shape of the body. At the start of a cycle, the resultant nodal forces are computed from the integration of stresses around each node and from external forces and the forces of interaction with other bodies. The current nodal accelerations are obtained from Newton's second law of motion and their integration yields the nodal velocities and the updated mesh. Incremental strains and rotations can be computed from the incremental displacements. Incremental stresses are then calculated from the constitutive law which employs Jaumann derivatives (Prager, 1961) to account for large deformation effects.

The last step in each cycle involves the computation of the forces of interaction at each node. The algorithm employed in PR3D is able to follow the development of the contact surfaces closely by monitoring the making and breaking of contacts at each node automatically. Once a node has been identified as intruding into another body, the normal component of the

incremental penetration, Δd, of the projectile node is computed. The components of the force of interaction, F_i, are calculated as

$$F_i = k(d + \Delta d)n_i \qquad (1)$$

where k is a user-specified contact stiffness, d is the total normal penetration, and n_i are the components of the surface normal. The force of interaction is applied to the node in the next cycle. An equal and opposite contact force is applied to the neighbouring body. This is distributed among the nodes of the element face through which the intruding node has penetrated. The manner of this distribution depends on the relative proximity of the intruding node and the nodes on the element face of the target body (Fig. 1). For a node-to-node contact, the contact force is applied to the nearest node only. For a node-to-edge contact, the force is distributed between the two nodes on that edge and for a node-to-face contact, the force is distributed among all three nodes.

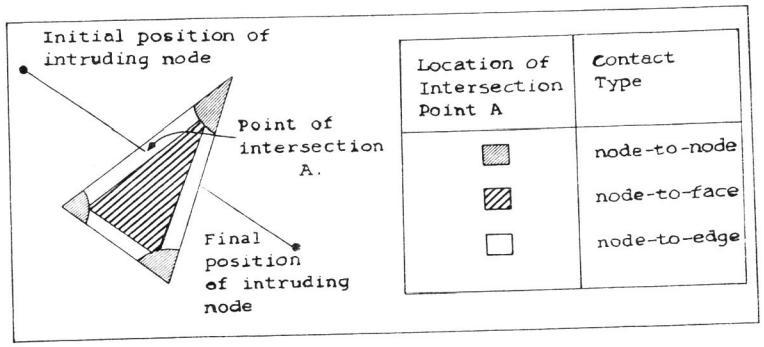

Fig. 1. Definitions of contact type

Nagtegaal, Parks and Rice (1974) have shown that due to the condition of local incompressibility, constant strain elements cannot model plastic flow accurately. To do this in PR3D, a mixed discretisation procedure (Marti and Cundall, 1982) has been incorporated. The deviatoric part of the strain tensor is calculated from the mesh of tetrahedron elements while the isotropic strains are referred to a mesh composed of larger elements, each consisting of up to six tetrahedrons.

SIMULATION OF FRACTURE

In general, any numerical technique which simulates the fracture of material and the subsequent material behaviour consists of two components. Firstly, a fracture criterion is required which defines the conditions necessary for fracture. This may be a function of stress or strain or a combination of

both. Secondly, there must be a procedure to represent the macroscopic behaviour of material after fracture has occurred. The two most common techniques either allow cracks to propagate between elements (Mackay, 1985; Rice and Sorensen, 1978) or represent fractured material as bands of elements with modified properties (Bazant and Cedolin, 1980; Mackay, Martin and Prinja, 1984; Wilkins, 1978).With the simplest of the fracture criteria used in both PR3D and HEMP, the normal components of the strain tensor in each element are checked during each cycle. If, in a particular element, one or more components exceed a critical value, which is specified by the program-user, that element is assumed to have fractured. A similar criterion in HEMP initiates fracture if either a critical stess or critical normal strain is exceeded.

Another criterion available in PR3D requires that

$$A\varepsilon_v + B\bar{\varepsilon}_p > 1 \qquad (2)$$

for fracture, where ε_v is the volumetric strain, $\bar{\varepsilon}_p$ is the effective plastic strain and A,B are material constants. In the above equation, 1/A is the volumetric strain at which the material will break under isotropic extension. Similarly, 1/B is the effective plastic strain when the material will fracture under conditions of constant volume. In strain space, the surface defined by (2), and formed by all the points at which the material fractures, is a cone of revolution around the isotropic axis. The apex is located at $\varepsilon_{xx} = \varepsilon_{yy} = \varepsilon_{zz} = 1/3A$. The intersection with the plane $\varepsilon_v = 0$ is a circle with radius 1/B plus the effective strain at yield.

A cumulative-strain-damage criterion has been proposed by Wilkins, Streit and Reaugh (1980). Fracture begins when the damage, D, exceeds a critical value over a critical distance and proceeds as the critical damage state is reached elsewhere. Damage is defined by the function

$$D = \int W_1 W_2 \, d\bar{\varepsilon}_p \qquad (3)$$

where W_1 is a hydrostatic-pressure weighting term and W_2 is an asymmetric-strain weighting term. Thus

$$W_1 = \left(\frac{1}{1 + ap} \right)^{\alpha} \qquad (4)$$

$$W_2 = (2-C)^{\beta} \qquad (5)$$

$$C = \mathrm{Max}\left(\frac{S_2}{S_3}, \frac{S_2}{S_1} \right) \qquad S_1 > S_2 > S_3 \qquad (6)$$

where p is the hydrostatic pressure; S_1, S_2, S_3 are the principal stress deviators; and a, α and β are material constants. This model is consistent with McClintock's theory of ductile fracture (1971) as it incorporates the influences of hydrostatic tension and asymmetric strain. Hydrostatic tension accounts for the growth of holes in fracture by spalling in which the loading consists of a large triaxial stress and small strain. The contribution of asymmetric strain accounts for the observation that the elongation before failure decreases as the shear load increases in fracture tests with combined loads. The damage function must be calibrated for a particular material using various material property tests. This was performed by Wilkins and co-workers (1980) for an aluminium alloy to simulate crack propagation in a compact tension specimen.

Of the two techniques for simulating the behaviour of fractured material, the procedure which allows cracks to propagate between elements is the more complex. As it requires that the propagation of cracks is traced explicitly, crack initiation, the direction of crack growth, crack branching and arrest need to be considered. The fracture process which follows impact between two solids does not necessarily commence from an initial crack. Clearly, this is not a simple task, especially in three dimensions. The alternative approach is far simpler and has been used by authors and their colleagues in both two- and three-dimensions. It has also been used by Bazant and Cedolin (1980) to simulate fracture in concrete.

Once an element is deemed to have fractured, its ability to transmit stresses must be modified. It is assumed in PR3D that material inside the element becomes a frictionless powder. Hence, it will not resist any deviatoric stresses and it will not withstand isotropic tension. However, the material is still present because, if compressed isotropically, it will continue to behave as if unfractured and because the mass of the fractured element remains lumped at the surrounding nodes.

The fracture of an element releases its stored elastic energy. Any stresses that the element was suffering, other than isotropic compression, disappear. Waves travel away from the fractured element carrying the released energy. The program reduces the instabilities that result from such an instantaneous energy release by reducing the stresses in the broken element gradually. From the instant of fracture, the flow stress and the maximum isotropic tension allowed in the element are halved every integration timestep. This is a very fast reduction (three orders of magnitude every ten timesteps) and experience has shown that it is adequate for avoiding instabilities.

When an element fractures and its stored energy is released, its neighbours will suffer additional deformation. If they are already very strained, that additional straining may be sufficient to fracture them. Even if the shock is not sufficiently high, there will be a stress redistribution caused by the effective hole created in the material for resistance purposes. The fracture will then propagate in a way similar to that of real fractures. Its velocity of propagation, though, may not be exactly the same because of the artificial rate of stress reduction.

SAMPLE PROBLEMS AND RESULTS

The following sections describe analyses performed by the authors and their colleagues involving impact between objects, fracture, penetration and perforation.

Inclined Impact of a Missile on Armour Plate

A missile moving with an axial velocity of 1360m/s hits an armour plate at an angle of incidence of 73^{O} (Principia, 1984). The missile is composed of a cylindrical body and a truncated conical nose with a half angle of 17^{O}, ended by a blunt cone. The material of the missile is stronger than that of the armour plate.

The computer program PR3D was used to analyse this problem. Due to symmetry, only half of the missile and armour plate was discretised using a mesh of 6870 tetrahedrons.

Plots showing the deformed shape of the missile and plate at 20, 60 and 130 μs after impact are shown in Figs. 2, 3 and 4 respectively. For clarity, brick elements representing six tetrahedrons are shown in the plot. The Figures show that, although the missile penetrates the armour plate initially, it eventually richochets from the plate.

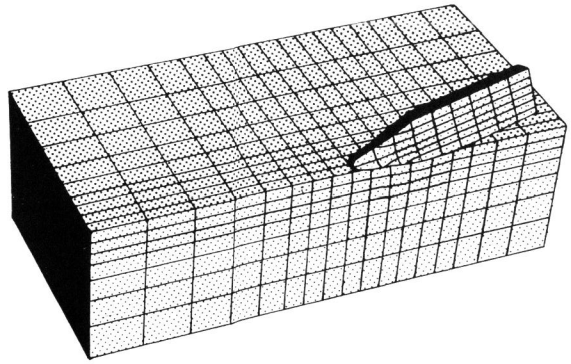

Fig. 2. Missile impact on armour plate after 20μs

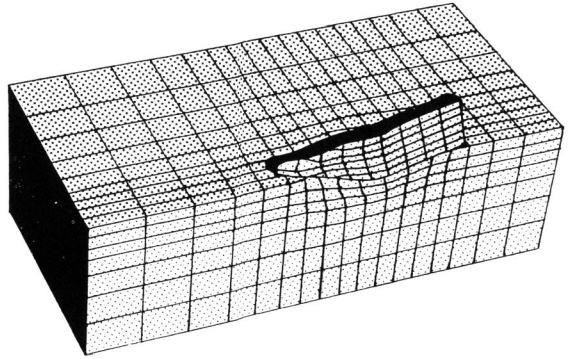

Fig. 3. Missile impact on armour plate after 60μs

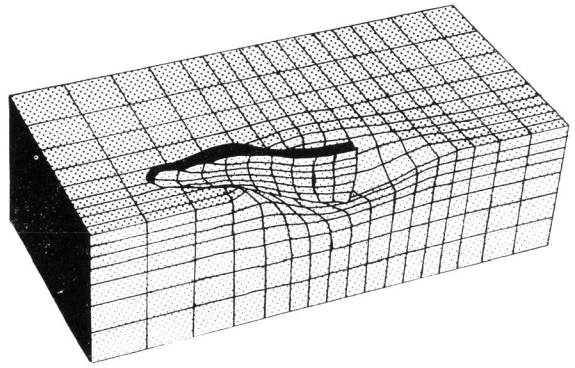

Fig. 4. Missile impact on armour plate after 130μs

Pipe-on-Pipe Impact

This example considers the impact between a stationary pipe and a whipping pipe (Mackay, Marti and Prinja, 1984) and demonstrates the behaviour of the method of simulating fracture used in PR3D. The stationary pipe was perfectly constrained at both ends and suddenly impacted at equal distances from its extremes by another pipe. This pipe, called the missile pipe, was free at its extremes and the impact took place also at equal distances from both ends. Both pipes were made from steel and were modelled as elastic-perfectly plastic with a Von Mises yield criterion. The whipping motion of the missile pipe was represented by prescribing an initial velocity of 50m/s vertically downwards.

Deformed meshes 5ms after impact are shown in Figs. 5 and 6 for two sets of pipes. With one set, the material did not rupture, while with the other, the material ruptured when any normal component of the strain tensor exceeded a critical value.

The analysis which used a rupture strain was identical to the non-rupturing analysis up to the point where strains reached the value of the critical rupture strain. Subsequently rupture started and caused the impact load to be smaller than in the non-rupturing case. As a consequence of rupture, the extent of the plastic zone in the target pipe was reduced. As elements fractured, further deformations were concentrated in the ruptured elements rather than in those undergoing plastic flow.

Normal Impact of a Missile on Armour Plate

The normal impact of a steel missile on an aluminium plate has been analysed axi-symmetrically using the computer program HEMP (Wilkins, 1978). The velocity of the projectile was 840m/s. Plots of the deformed shape of the missile and plate are compared with experimental results in Fig. 7. The calculated time for the penetration and the missile exit velocity agree with the experiment.

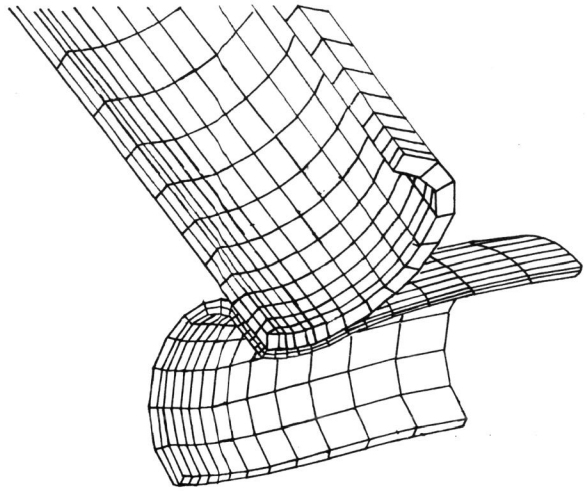

Fig. 5. Pipe-on-pipe impact after 5ms - non-rupturing material

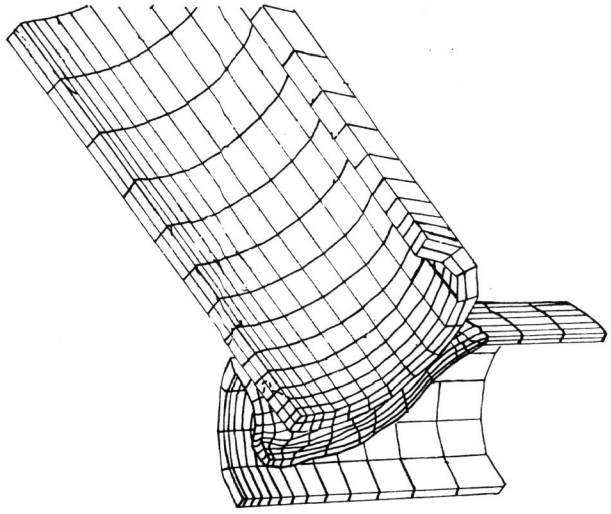

Fig. 6. Pipe-on-pipe impact after 5ms - rupturing material

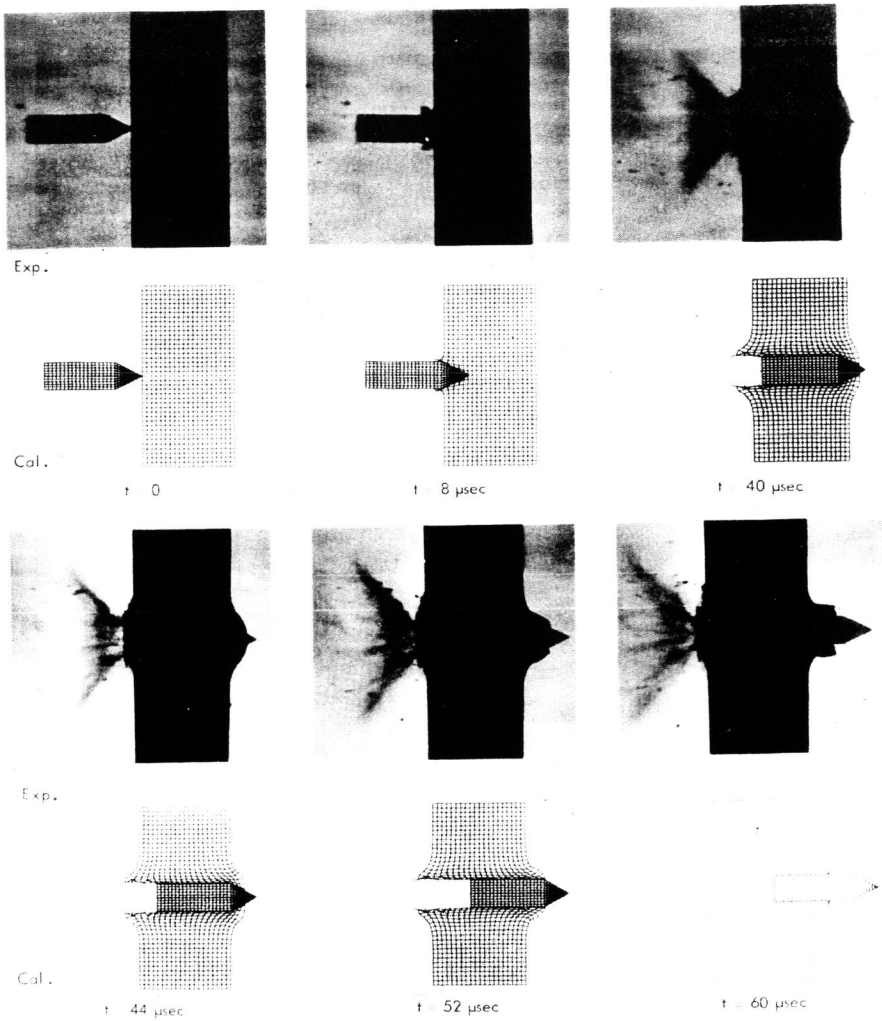

Fig. 7. Experiment and calculation of a steel projectile penetrating an aluminium plate

Since the strength of the projectile is greater than that of the plate, the projectile does not deform and its nose remains pointed. Hence, a high stress occurs ahead of the missile which overcomes the shear strength of the plate. Thus penetration occurs by radial flow of material in the aluminium plate ahead of the projectile. The material property which controls the behaviour of the plate is its shear strength. Consequently when this property was altered, neither the computed penetration time nor the exit velocity agreed with the experiment.

Impact of a Spherical Ram on an Aluminium Plate

This analysis, also performed with HEMP, considers the impact of a spheri ram moving at 900m/s onto a thin aluminium plate (Wilkins, 1978). Fractu was permitted when either a critical stress or a critical normal strai component was exceeded. Large hoop stresses were generated along the axis symmetry in the plate and fracture initiated on the surface opposite impa (Fig. 8). This was also observed experimentally and is called petaling a fracture propagates through the thickness of the plate and radially, formi triangular petals.

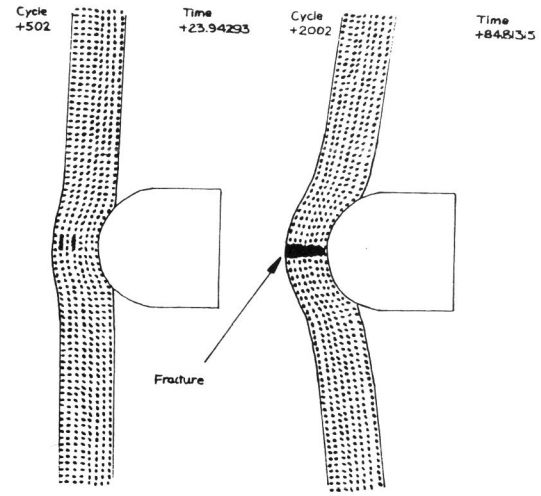

Fig. 8. Calculated penetration of an aluminium target by a spherical steel ram.

The projectile diameter to plate thickness ratio determines whether failure is by petaling or plugging. When this is greater than unity, as in this example, failure is by petaling. If the plate thickness is increased, the plate stiffness increases faster than the bending stress. On the other hand, large shear stresses are now set up around the perimeter of the missile and failure occurs in this region instead. This is known as plugging and occurs in the example described in the next section.

Perforation of a Plate by a Punch

The perforation of a thin mild steel plate by a flat headed, rigid cylindrical projectile has been analysed using PR3D. The plate was rigidly supported around its circumference. Its material behaviour was modelled as elasto-plastic with power law hardening and the fracture criterion was defined by equation (3). As only limited experimental data was available, it was necessary to adopt values for the constants A and B. It was assumed that, under constant volume, fracture would occur at effective plastic

strains of 40%, while fracture under purely volumetric deformation would occur at a strain of 60%. The velocity of the punch was 7.6 m/s and was held constant during penetration.

A 60° segment of the plate and projectile was idealised using tetrahedral elements. There were 1368 elements in the plate, with two layers of elements through its thickness, and 72 tetrahedra in the punch. A hidden line view of the mesh in shown in Fig. 9.

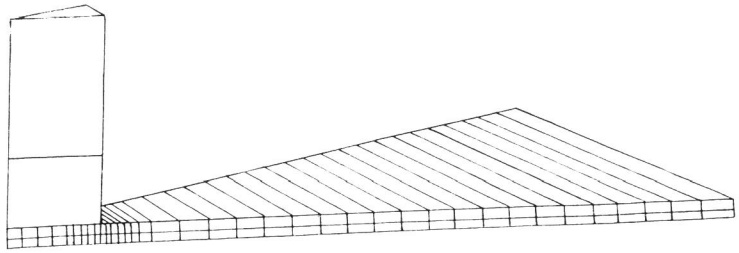

Fig. 9. Mesh used to analyse perforation of a plate by a punch

The propagation of rupture is shown in Fig. 10, where shaded areas represent locations where both layers of elements have failed. Elements in contact with the punch started failing at 2.3μs after impact while by 11.5μs a complete annulus of elements had ruptured.

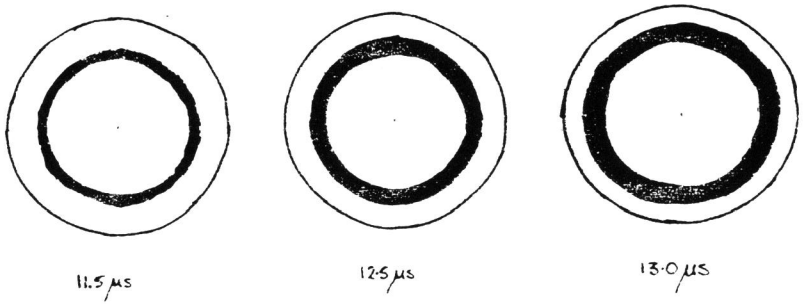

Fig. 10. Propagation of rupture during penetration of a plate by a punch

The cylindrical punch creates a large shear stress on a surface which surrounds a plug of material under the punch. The gradual increase of this stress results in yield and eventually fracture of the material. Our results show that this will occur first on the top layer of a ring of elements under the perimeter of the punch. Additional motion of the punch transfers the failure zone further into the plate until the full thickness of the plate has fractured.

The maximum impact force was 32kN. An analytical solution estimates the maximum force required to penetrate a plate as (Goldsmith, Liu and Chulay, 1965)

$$F_{max} = 2 \pi R \tau h \qquad (7)$$

where R is the radius of the punch, h is the plate thickness and τ is its yield stress in shear. For the problem under consideration here, F_{max} is 10.1kN which, although of the same order of magnitude as the numerical value, differs by a factor of about 3. This most probably occurred because of several simplyfying assumptions in the analytical solution which were unnecessary in our computations. For example, in Goldsmith, Liu and Chulay (1965) it was assumed that the material was elastic-ideally-plastic while our analysis permitted strain hardening. If the ultimate strength, instead of the yield strength, of the material was used in (7), the predicted load would increase by 60%. In addition, our computations allowed fracture of the material and also followed the non-linear vibrations introduced by the impact, which cannot be accounted for by (7).

Perforation of a Roof Plate by a Pipe-End

This analysis investigated the effects of impact of the end of a whipping pipe on a roof plate. As a consequence of the rotation of the pipe about its restrained end, the velocity of its free end contained components which were both normal and tangential to the roof plate. At impact, the former was equal to 90m/s.

The material of both the pipe and plate was mild steel and was represented by an elasto-plastic law with Von Mises yield criterion and isotropic hardening. The latter was described by a power law. The failure criterion and the values of the constants A and B were the same as in the previous example.

The mesh representing the pipe consisted of 960 tetrahedral elements while the plate was modelled with two layers of 3872 tetrahedrons in each layer. Fig. 11 shows the mesh near to the point of impact where obviously the refinement of the mesh is increased. For clarity, Fig. 11 only shows brick elements - each brick element is, in fact, composed of six tetrahedrons.

The analysis was performed up to 75μs after impact. At about 60μs, elements started to rupture. Fig. 12 shows the situation at 71μs. Fractured elements have been removed from the plot to ease visualisation. From the Figure, it is clear that the pipe has perforated the plate. As the free-end of the pipe is moving across the plate, the maximum dimension of the ruptured region is also in that direction.

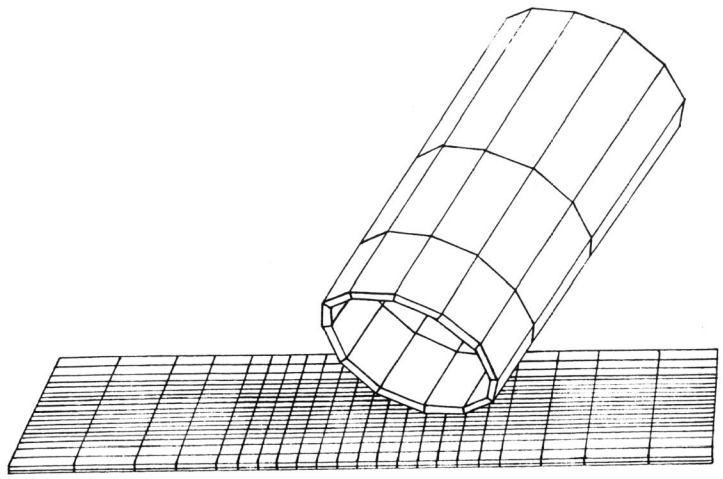

Fig. 11. Detail of mesh used to analyse perforation of a roof plate by a pipe

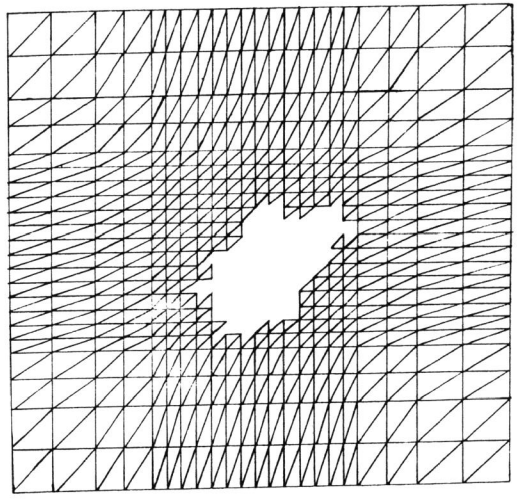

Fig. 12. Perforated roof plate 71μs after impact by a pipe

The deformations of the pipe, by comparison with those of the plate, were very small. This is a consequence of the stiffness afforded by the geometry of the pipe.

CONCLUSIONS

We have described the numerical techniques that are necessary to model the fracture mechanisms associated with impact, penetration and perforation. A number of examples showed both the insight that can be gained into theoretical aspects of such problems and also demonstrated practical applications of these procedures. Clearly, for further advances in this field, there is a need for greater experimental data than is presently available in order to define more precisely the parameters characterising fracture of materials under conditions of dynamic loading.

ACKNOWLEDGEMENTS

The pipe-on-pipe impact analyses were funded by National Nuclear Corporation Limited, U.K. The authors are grateful to Drs. Kalsi, Mackay, Marti and Trbojevic for performing the numerical analyses which used PR3D and for preparation of this paper.

REFERENCES

Bazant, Z.P., and L. Cedolin (1980). Fracture mechanics of reinforced concrete. Proceedings A.S.C.E., Engineering Mechanics Division, 106, 1287-1306.

Goldsmith, W., T.W. Liu and S. Chulay (1965). Plate impact and perforation by projectiles. Experimental Mechanics, 385-404.

Johnson, W. (1972). Impact Strength of Materials. Edward Arnold, London.

Mackay, D.C.(1982). Finite element investigation of general yield fracture. Ph.D. Thesis, C/Ph/68/82, University of Wales, U.K.

Mackay, D.C., J. Marti and N.K. Prinja (1984). Three-dimensional analysis of pipe-on-pipe impact and fracture. In A.R. Luxmoore and D.R.J. Owen (Eds.), Third International Conference on Numerical Methods in Fracture Mechanics, Swansea.

Marti, J., and P.A. Cundall (1982). Mixed Discretisation Procedure for Accurate Modelling of Plastic Collapse. International Journal for Numerical and Analytical Methods in Geomechanics, 6, 129-139.

McClintock, F.A. (1971). Plasticity Aspects of Fracture. In H. Liebowitz (Ed.), Fracture, an Advanced Treatise. Academic Press, New York-London.

Nagtegaal, J.C., D.M. Parks and J.R. Rice (1974). On numerically accurate finite element solutions in the fully plastic range. Comput. Methods Appl. Mech. & Eng., 4, 153-177.

Prager, W. (1961). An elementary discussion of definitions of stress rate. Q. appl. Math., 18, 403-407.

Principia Mechanica Ltd. (1983). PR3D documentation. Report Nos. PR-TN-4 to PR-TN-7, Version 3P-2, London.

Principia Mechanica Ltd. (1984). 78^{O} impact of a missile on armour plate. Technical Note PR-TN-21, London.

Rice, J.R., and E.P. Sorensen (1978). Continuing crack-tip deformation and fracture for plane-strain crack growth in elastic-plastic solids. Journal of Mechanics and Physics of Solids, 26, 163-186.

Wilkins, M.L. (1969). Calculation of elastic-plastic flow. Lawrence Livermore Report UCRL-7322, Rev. I., Livermore, California.

Wilkins, M.L. (1978). Mechanics of penetration and perforation. International Journal of Engineering Science, 16, 793-807.

Wilkins, M.L., R.D. Streit and J.E. Reaugh (1980). Cumulative-strain-damage model of ductile fracture: simulation and prediction of engineering fracture tests. Lawrence Livermore Laboratory Report No. UCRL-53058, Livermore, California.